SolarPACES 2022, 28th International Conference on Concentrating Solar Power and Chemical Energy Systems
Measurement Systems, Devices, and Procedures
https://doi.org/10.52825/solarpaces.v1i.724

Published: 15 Mar. 2024

# Device for Measuring Forces and Torques in Flexible Connection Joints for Parabolic Trough Collector

Rafael López-Martín[1][https://orcid.org/0000-0003-0170-9209], Loreto Valenzuela[1][https://orcid.org/0000-0001-9505-8333], and Carmen M. Amador-Cortés[1][https://orcid.org/0000-0002-1121-6750]

[1] CIEMAT-Plataforma Solar de Almería, Spain

**Abstract.** Measurement of forces and torques in flexible connection joints for parabolic trough collectors (PTC) during their life time is important to prevent damage or breakage of these elements. Plataforma Solar de Almería (PSA) has developed and patented a device for measuring these forces and torques in flexible connection joints installed in solar power plants. The device consists of three dynamometers and one torque transducer coupled to a rotation assembly that can be externally coupled to a ball joint installed in interconnections of parabolic-troughs, with no interference in the hydraulic circuit. To calibrate the device and perform initial performance checks at lab scale, a test bench was prepared for applying forces and torques on a set-up composed of a multicomponent sensor connected in series to a standard rotary ball joint and measuring simultaneously the forces and torques by mean of the designed device. Calibration tests have been performed applying a range of forces and torques to the multicomponent sensor-ball joint at different rotation positions. Multicomponent sensor and developed device measurements have been compared to obtain a calibration matrix for the last one. Results show good performance of the device once calibrated, but that will be improved measuring angular deviations from reference axes position of each of the dynamometers that compose the device during the operation, to increase the accuracy of the measurements.

**Keywords:** Solar Thermal Energy, Parabolic Troughs, Rotation and Expansion Performing Assemblies, Flexible Hose, Swivel Joint, Forces, Torques

## 1. Introduction

Flexible connection joints for parabolic trough collectors (PTC) are one of the critical components in PTC solar fields. These elements connect the inlet and outlet receiver tubes between collectors installed in series in the solar field or between the inlet/outlet of the moving receivers and the fixed process pipes. During their life time, these components suffer wear due to relative movement of piping that they connect by the rotation movement of the collector or by thermal expansion of the receivers. The damage or breakage of these elements causes significant economic damage to the solar plant, not only because of the cost of these elements or the heat transfer fluid (HTF) lost due to leaks, but also because the operation of the affected collectors is stopped, decreasing energy production. In addition, dangerous situations can occur due to leakage, with soil contamination, toxic clouds and in the worst case triggering a fire [1]. Knowing the forces and torques on the flexible joint during the operation gives information about the performance evolution and wear of the joint.

Plataforma Solar de Almería (PSA) has developed and patented a device for measuring forces and torques in flexible connection joints for parabolic trough collectors during the operation of this key component in solar power plants [2]. The main features and details of its operation are described in this article.

## 2. Methodology

The force and torque measuring device for flexible connection joints installed in PTC solar fields (see Figure 1a), called SOLDYN, has been developed and built at the PSA. The device is designed to be coupled to the piping where there is a swivel or ball joint installed.

### 2.1. Description of the measuring device

SOLDYN, consists of three dynamometers and one torque transducer. The torque transducer (labelled as #1 in Figure 1b) is installed in the connection of the collector rotation axis with the joint rotation axis. Dynamometers are mounted in a steal structure fixed to the inlet and the outlet pipe of the rotary ball joint. One of the dynamometers for measuring forces (#2, Figure 1b) is connected parallel to the rotation axis of the joint and the other two (#3 and #4, Figure 1b) are perpendicular to the main rotation axis.

Torque transducer used (#1) is a model AEP-MTRX2KNM005 manufactured by AEP Transducers®, connected to an amplifier AEPETAD4111D24 from the same manufacturer. This torque transducer let measure a range of 2000Nm around the two directions and precision class 0.05. Dynamometer used for measure forces parallel to rotation axis (#2) is a model AEP-CTCA1K5 manufactured by AEP Transducers®, connected to an amplifier model AEP-ETA4D211D24 from the same manufacturer. This dynamometer has a measure range of 10N in both directions and precision class 0.1. Dynamometers used for measure forces perpendicular to rotation axis (#3 and #4) are model 1-S2M/10N-1 manufactured by HBM®, connected to two amplifiers model AE 301 from the same manufacturer. These dynamometers have a measure range of 10N in both directions and precision class 0.02.

A split bearing (#5, Figure 1b) is installed on the axis of the fixed process piping to let the rotation of the system. This kind of bearing allows the installation of the device around the process piping without interference to the joint because can be dismounted in two half pieces. The bearing has been insulated regarding the process pipe when it is mounted.

(a)

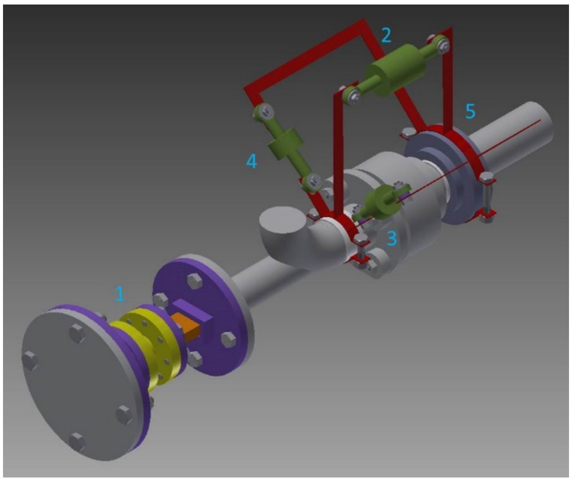


(b)

**Figure 1**. Device for measuring forces and torques in flexible connection joints for PTCs: (a) Device installed in the outlet of a parabolic trough collector, (b) sketch.

The torque transducer measures the moment ($M_z$) on the ball joint in the main rotation axis direction (labelled as #1 in Figure 1b). Dynamometers #3 and #4 measure forces ($F_x$ and $F_y$, respectively) perpendicular to rotation axis, and dynamometer #2 measures force ($F_z$) parallel to rotation axis. Torque in the rotary ball joint in the parallel axis to dynamometer #3 ($M_x$) is calculated as the product of force measured by dynamometer #4 ($F_y$) by the distance ($d$) of this axis to dynamometer #4.

$$M_x = F_y * d \tag{1}$$

In the same way, torque in the rotary ball joint in the parallel axis to dynamometer #4 ($M_y$) is calculated as the product of force measured by dynamometer #3 ($F_x$) by the distance ($d$) of this axis to dynamometer #3.

$$M_y = F_x * d \tag{2}$$

Measured data are registered by mean of a supervisory control and data acquisition system (SCADA), developed in Labview software and running in a PC. Functionalities implemented in this SCADA are online monitoring and recording of measured data by the different sensors, and possibility of initialization to zero of the different measurements.

## 2.2. Description of the experimental set-up for calibration

To perform the calibration of the SOLDYN device, the system has been installed in a test bench where a calibrated multicomponent sensor is also installed (see Figure 2), and a comparison test campaign has been performed. Multicomponent sensor is a model K-MCS10-100-6C-FX-FY-FZ-MX-MY-MZ with amplifier model 1-BM40IE ClipX, both manufactured by HBM®. This multicomponent sensor is of accuracy class 0.1 with measurement ranges $F_x$=20kN, $F_y$=20kN, $F_z$=100kN, $M_x$=2kN·m, $M_y$=2kN·m and $M_z$=1.5kN·m, all of them in both directions.

The test bench is prepared to allow applying forces and torques on a standard rotary ball joint. The multicomponent sensor has been installed in a position comparable to the rotary ball joint position, and in series to a ball joint, and SOLDYN in the defined measuring position as presented in Figure 1a. A rotary ball joint is included in this experimental set-up to allow the rotation of the system and then achieve representative mechanical positions to make the measures.

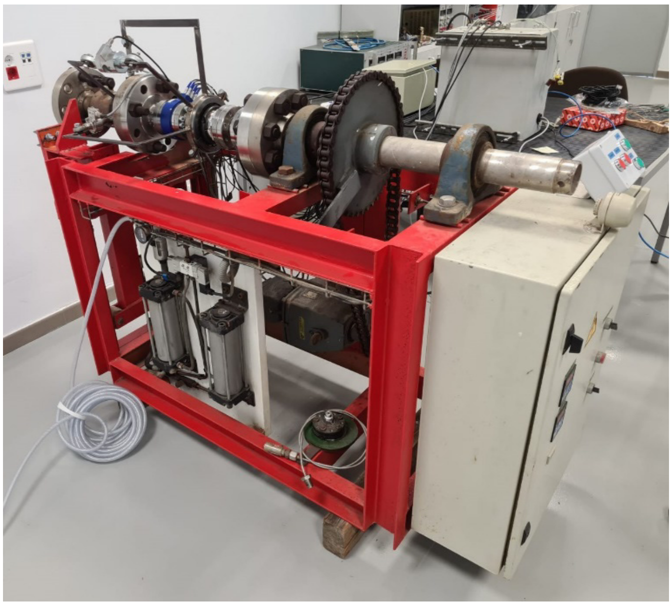

**Figure 2**. Calibration test bench of the device for measuring forces and torques in flexible connection joints.

To simplify the calculation, SOLDYN has been installed with its x, y and z axes parallel to the respective axes of the multicomponent sensor. The test bench is prepared to allow applying forces perpendicular to the floor using a pneumatic piston, and let the rotation in the axis of the rotary ball joint.

## 2.3. Test procedure for calibration

Forces and torques are applied on the ball joint and multicomponent sensor using different expansion lengths of the pneumatic piston (~0mm, ~5mm, ~10mm, ~15mm), for different axis directions (x,y,z) by rotating the system (0°, 30°, 45°, 60°, 90º). The multicomponent sensor measurements ($F_{x,M}$,$F_{y,M}$,$F_{z,M}$,$M_{x,M}$,$M_{y,M}$,$M_{z,M}$), which are the reference forces and moments that are actually being applied in the ball joint, and the ones provided by the SOLDYN device ($F_{x,S}$,$F_{y,S}$,$F_{z,S}$,$M_{x,S}$,$M_{y,S}$,$M_{z,S}$) are compared to obtain a calibration matrix (Eq. 3), which is later used to correct the measurements provided by the SOLDYN device once installed and measuring in the solar field and calculate the actual forces and torques in the ball joint.

$$\begin{pmatrix} F_{x,M} \\ F_{y,M} \\ F_{z,M} \\ M_{x,M} \\ M_{y,M} \\ M_{z,M} \end{pmatrix} = \begin{pmatrix} a_{1,1} & a_{1,2} & a_{1,3} & a_{1,4} & a_{1,5} & a_{1,6} \\ a_{2,1} & a_{2,2} & a_{2,3} & a_{2,4} & a_{2,5} & a_{2,6} \\ a_{3,1} & a_{3,2} & a_{3,3} & a_{3,4} & a_{3,5} & a_{3,6} \\ a_{4,1} & a_{4,2} & a_{4,3} & a_{4,4} & a_{4,5} & a_{4,6} \\ a_{5,1} & a_{5,2} & a_{5,3} & a_{5,4} & a_{5,5} & a_{5,6} \\ a_{6,1} & a_{6,2} & a_{6,3} & a_{6,4} & a_{6,5} & a_{6,6} \end{pmatrix} \cdot \begin{pmatrix} F_{x,s} \\ F_{y,s} \\ F_{z,s} \\ M_{x,s} \\ M_{y,s} \\ M_{z,s} \end{pmatrix} \tag{3}$$

To obtain parameters $a_{i,j,}$ multiple linear regressions have been done by means of software OriginPro 2021©. To compare and check the influence of the rotation angle fits were repeated for each one. The measurement uncertainties have been calculated following the Guide to the Expression of Uncertainty in Measurement (GUM) (1995) [3].

# 3. Results

To resume the results of the different fits performed, one of the obtained calibration matrices ($A_{0^\circ}$) in the calibration test applying a rotation angle of 0 degrees, is detailed next (Eq. 4). Additional calibration matrices $A_{30^\circ}$, $A_{45^\circ}$, $A_{60^\circ}$ and $A_{90^\circ}$ were obtained for each rotation angle.

$$A_{0^\circ} = \begin{pmatrix} 3\cdot 10^4 & -26\cdot 10^4 & 17.6 & 175\cdot 10^4 & -20\cdot 10^4 & -6.66 \\ -26\cdot 10^4 & -36\cdot 10^4 & -534 & 24\cdot 10^5 & 18\cdot 10^5 & -19.4 \\ 17\cdot 10^4 & 38\cdot 10^4 & 403 & -25\cdot 10^5 & -12\cdot 10^5 & 1.79 \\ -1\cdot 10^5 & -0.9\cdot 10^5 & -342 & 6\cdot 10^5 & 6\cdot 10^5 & -6.03 \\ 1\cdot 10^3 & 38\cdot 10^3 & 3.4 & -25\cdot 10^4 & -4\cdot 10^3 & 1.44 \\ 16\cdot 10^2 & 62\cdot 10^2 & 7.74 & -41\cdot 10^3 & -11\cdot 10^3 & 1.1728 \end{pmatrix} \tag{4}$$

Figure 3 shows graphical results of the comparison among forces and torques directly measured by the multicomponent sensor installed in line with a ball joint (MS, red dots, in the graphs), and the calculated forces and torques multiplying the calibration matrix (Eq.4) by the SOLDYN device measurements ($F_{x,S}$,$F_{y,S}$,$F_{z,S}$,$M_{x,S}$,$M_{y,S}$,$M_{z,S}$) (blue dots in the graphs). Results include uncertainty bounds.

Uncertainties calculated for the SOLDYN device measurements are slightly larger to the ones of the multicomponent sensor, what is due to the combined uncertainty of the individual measurements of the sensors included in SOLDYN and that of the adjusted calibration matrix.

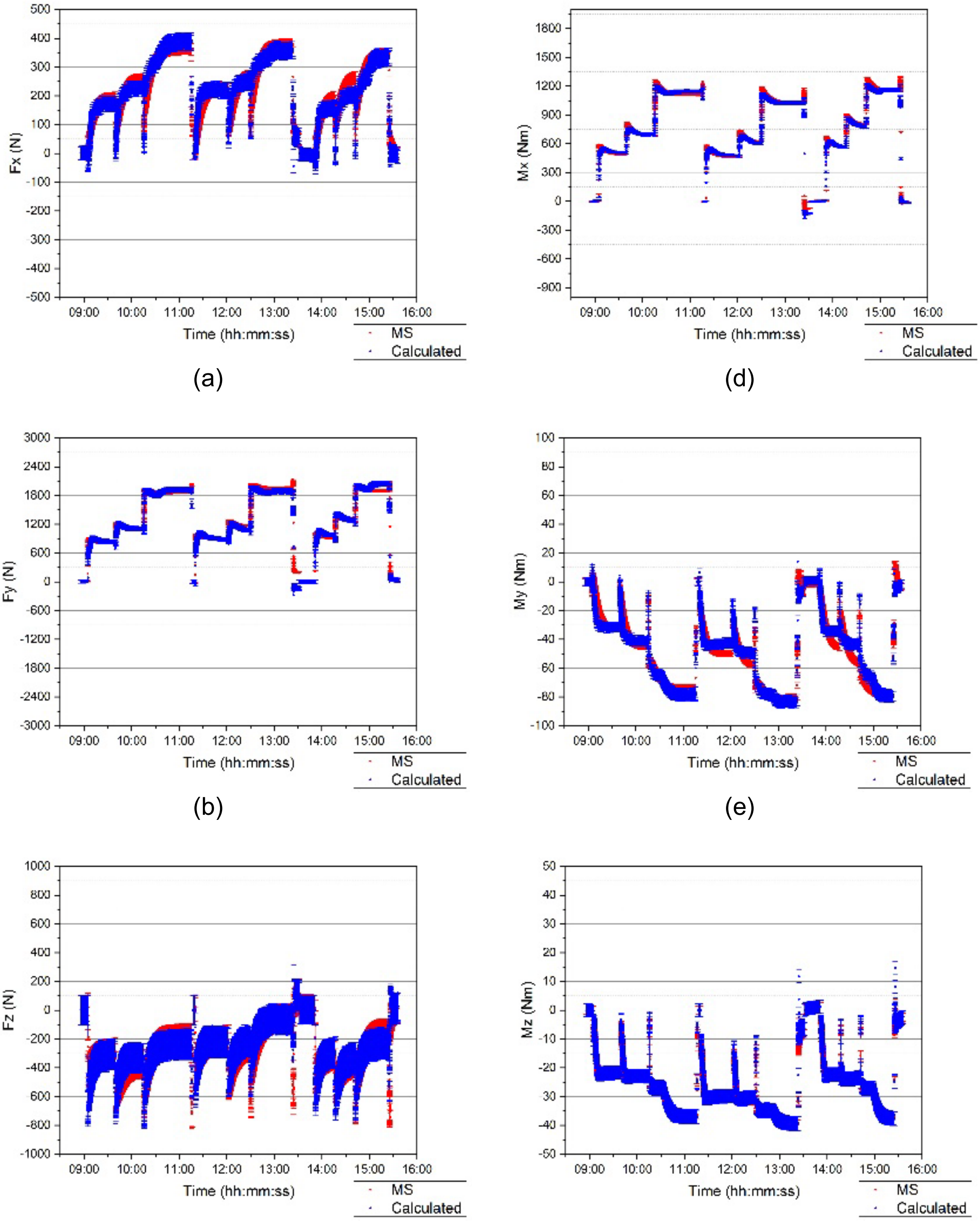


**Figure 3**. Comparison of multicomponent sensor (MS) and SOLDYN measurements (forces and torques) considering the calculated calibration matrix for 0°: (a) $F_x$, (b) $F_y$, (c) $F_z$, (d) $M_x$, (e) $M_y$, (f) $M_z$.

Some of the graphs include two different values of forces and moments at the same time period; this is because some tests were repeated on different dates and are represented in the same graph to simplify and compare to other results obtained for the same rotation angle. It is also seen that when an expansion length of the pneumatic piston is reached the system takes few minutes to reach steady state in forces and torques, which is also relevant information to quantify time response of the system.

From the regression analyses performed, calibration matrices obtained showed different coefficients depending on the rotation angle, what demonstrate the influence of this parameter during the measurement process.

To quantify the good quality of the fits, r-square ($R^2$) values of the adjustment performed for each rotation angle of the system (0°, 30°, 45°, 60°, 90º), are shown in Table 1:

**Table 1.** Results for $R^2$ fit parameter for each rotation angle during the calibration process.

| | **0°** | **30°** | **45°** | **60°** | **90°** |
|---|---|---|---|---|---|
| $F_x$ | 0.9873 | 0.9847 | 0.9932 | 0.9898 | 0.9919 |
| $F_y$ | 0.9945 | 0.9897 | 0.9911 | 0.9734 | 0.9876 |
| $F_z$ | 0.9615 | 0.7522 | 0.7611 | 0.7857 | 0.9273 |
| $M_x$ | 0.9971 | 0.9978 | 0.9970 | 0.9881 | 0.9854 |
| $M_y$ | 0.9876 | 0.9944 | 0.9973 | 0.9984 | 0.9954 |
| $M_z$ | 0.9992 | 0.9985 | 0.9980 | 0.9976 | 0.9981 |

A set of additional tests were executed in the test bench to verify the good quality of the calibration performed. As tests previously done for the calibration tests, these new tests consisted in applying four different expansion lengths by mean of the pneumatic piston in three different time periods and measuring the corresponding forces and torques. Tests were also repeated for each rotation angle. Figures 4 to 6 shows the comparative of results between multicomponent sensor (MS) and SOLDYN (Calculated) measurements for different rotation angles: 0, 45, and 90 degrees respectively. The calculated values are obtained applying the corresponding calibration matrices obtained during the calibration process; in the case of rotation angle equal to 0 degrees the calibration matrix considered is Eq. 4. Results shown include uncertainty bounds.

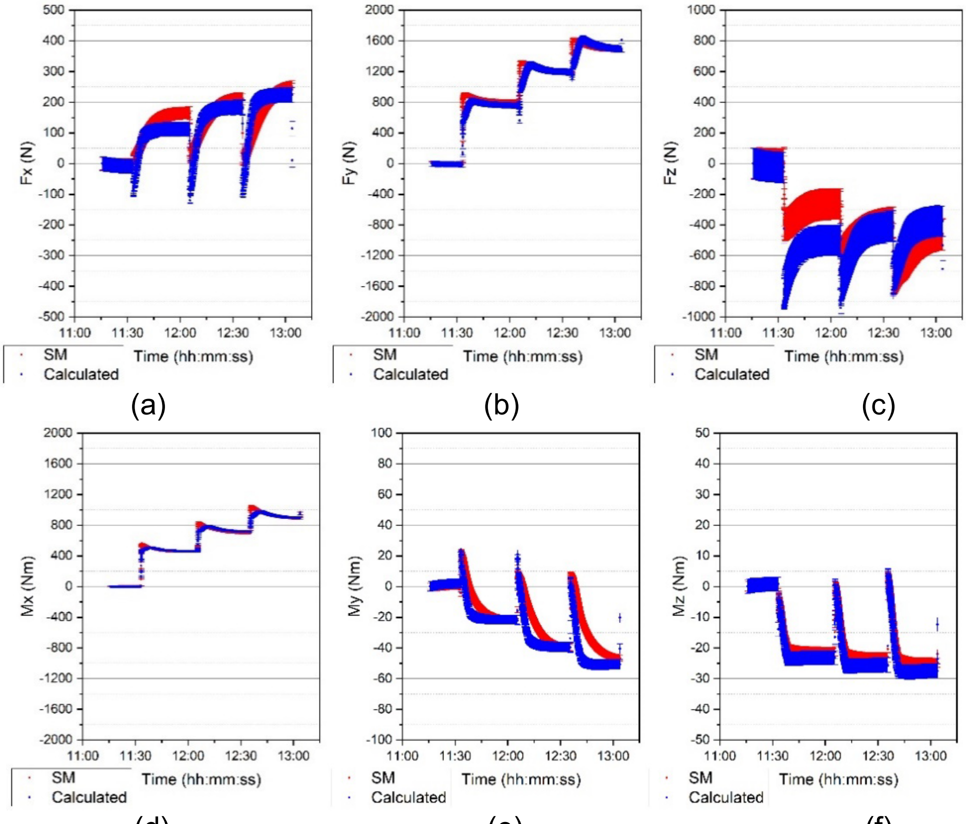


**Figure 4**. Comparison of multicomponent sensor (MS) and SOLDYN measurements considering the calculated calibration matrix for 0°: (a) $F_x$, (b) $F_y$, (c) $F_z$, (d) $M_x$, (e) $M_y$, (f) $M_z$.

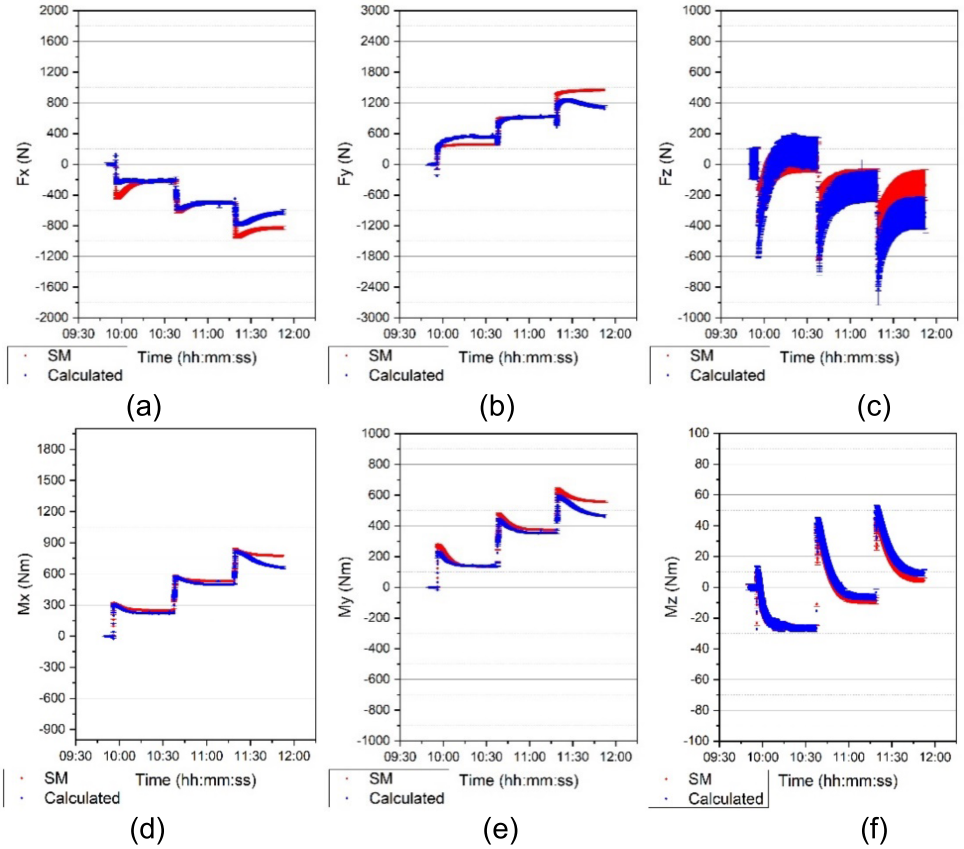

**Figure 5**. Comparison of multicomponent sensor (MS) and SOLDYN measurements considering the calculated calibration matrix for 45°: (a) $F_x$, (b) $F_y$, (c) $F_z$, (d) $M_x$, (e) $M_y$, (f) $M_z$.

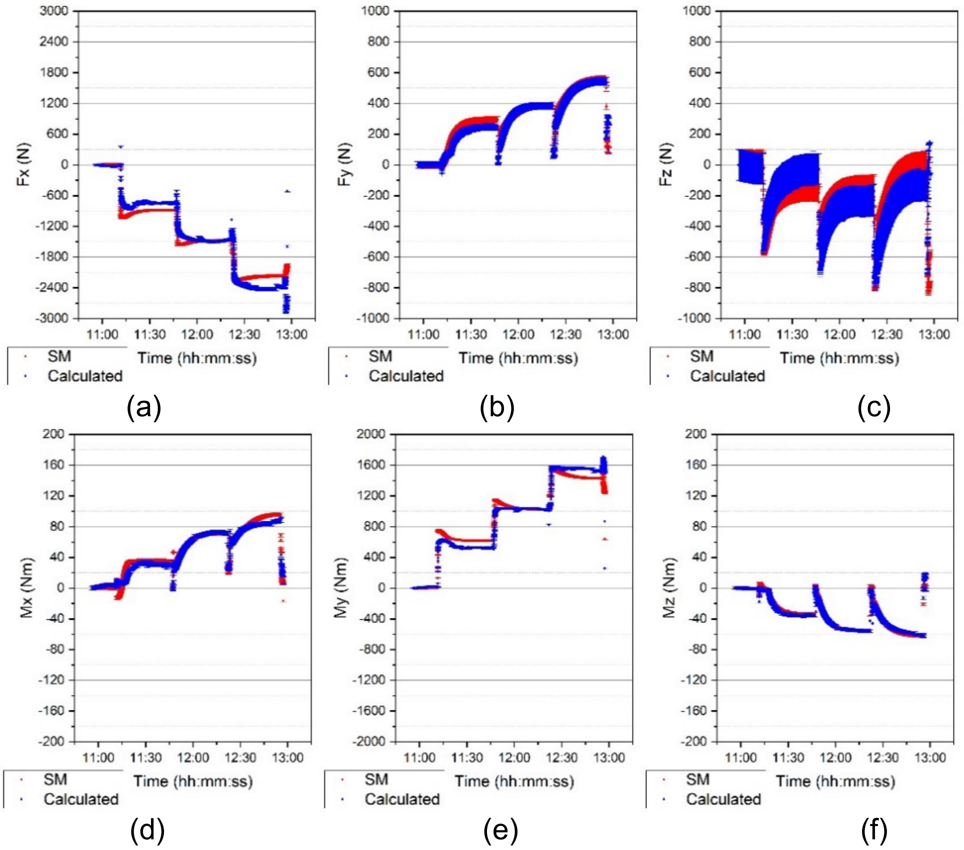

**Figure 6**. Comparison of multicomponent sensor (MS) and SOLDYN measurements considering the calculated calibration matrix for 90°: (a) $F_x$, (b) $F_y$, (c) $F_z$, (d) $M_x$, (e) $M_y$, (f) $M_z$.

## 4. Discussion

In general, calibration matrices fitting results are considered very good. The worst results correspond to the fitting of $F_z$ force. A possible explanation is that the dynamometer measuring this component of the force in SOLDYN device, which is installed parallel to the longitudinal rotation axis direction, is deviated by the movement of pneumatic piston. Due to this, it has been concluded the need of measuring any angular deviation of the dynamometers from their corresponding main axis to add an additional correction to the forces measured by SOLDYN. This will be an improvement that will be implemented in the near future.

In addition, this first calibration of the SOLDYN device has also demonstrated there is a high dependence with the rotation angle of the system. To manage this issue, it is needed to measure the rotation angle and the deviation on the direction of any of the dynamometers during a test. This will be an improvement that will be implemented in the near future. It has been verified that when calibration matrix is considered to calculate the forces and torques in the rotary ball joint from SOLDYN data, results are very similar to the ones measured by the multicomponent sensor. For rapid movements, results presented show some deviations due to the different times response of SOLDYN sensors and multicomponent sensor. However, results are equivalent in steady state.

Future work will also consist in the installation of the SOLDYN device in a flexible interconnection joint of a parabolic-trough collector of one of the pilot plants at PSA. Experimental work will continue to check the performance of the measurement device.

## Data availability statement

Datasets of results presented are available through: https://doi.org/10.5281/zenodo.7005152.

## Author contributions

Conceptualization, R.L.M., L.V.; Resources: R.L.M., L.V., C.A.C.; Methodology, R.L.M., L.V.; Data curation, R.L.M., L.V.; Validation, R.L.M., L.V.; Writing – original draft, R.L.M.; Writing – review & editing, L.V., C.A.C.

## Competing interests

The authors declare no competing interests.

## Acknowledgement

This work has received funding from the European Union's Horizon 2020 research and innovation program under grant agreement No. 823802 (SFERA-III).

## References

1. H. Price and D. Kearney, "Reducing the Cost of Energy from Parabolic Trough Solar Power Plants" ASME 2003 International Solar Energy Conference, ISEC2003-44069, pp. 591-599, 2009. https://doi.org/10.1115/ISEC2003-44069
2. R. López-Martín, L. Valenzuela, Spanish patent ES 2788802B2 (2021).
3. GUM, Guide to the Expression of Uncertainty in Measurement. Working group convened by experts of: Bureau International des Poids et Mesures (BIPM), International Electrotechnical Commission (IEC), International Organization of Legal Metrology (OIML), 1995.